ACCOUNTS
of chemical research

Multifunctionality of Organometallic Quinonoid Metal Complexes: Surface Chemistry, Coordination Polymers, and Catalysts

SANG BOK KIM,*,†,§ ROBERT D. PIKE,‡ AND DWIGHT A. SWEIGART†,∥

†Department of Chemistry, Brown University, Providence, Rhode Island 02912, United States, ‡Department of Chemistry, The College of William & Mary, Williamsburg, Virginia 23187, United States, and §Department of Chemistry & Chemical Biology, Harvard University, Cambridge, Massachusetts 02138, United States

RECEIVED ON JANUARY 20, 2013

CONSPECTUS

Quinonoid metal complexes have potential applications in surface chemistry, coordination polymers, and catalysts. Although quinonoid manganese tricarbonyl complexes have been used as secondary building units (SBUs) in the formation of novel metal−organometallic coordination networks and polymers, the potentially wider applications of these versatile linkers have not yet been recognized. In this Account, we focus on these diverse new applications of quinonoid metal complexes, and report on the variety of quinonoid metal complexes that we have synthesized.

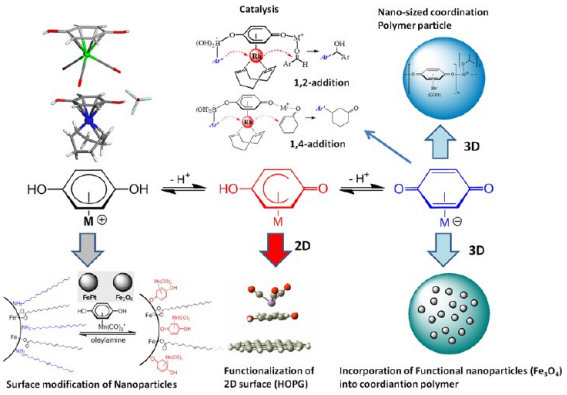

Through the use of $[(\eta^6\text{-hydroquinone})Mn(CO)_3]^+$, we are able to modify the surface of Fe_3O_4 and FePt nanoparticles (NPs). This process occurs either by the replacement of oleylamine with neutral $[(\eta^5\text{-semiquinone})Mn(CO)_3]$ at the NP surface, or by the binding of anionic $[(\eta^4\text{-quinone})Mn(CO)_3]^-$ upon further deprotonation of $[(\eta^5\text{-semiquinone})Mn(CO)_3]$ at the NP surface. We have demonstrated chemistry at the intersection of surface-modified NPs and coordination polymers through the growth of organometallic coordination polymers onto the surface modified Fe_3O_4 NPs. The resulting magnetic NP/organometallic coordination polymer hybrid material exhibited both the unique superparamagnetic behavior associated with Fe_3O_4 NPs and the paramagnetism attributable to the metal nodes, depending upon the magnetic range examined. By the use of functionalized $[(\eta^5\text{-semiquinone})Mn(CO)_3]$ complexes, we attained the formation of an organometallic monolayer on the surface of highly ordered pyrolitic graphite (HOPG). The resulting organometallic monolayer was not simply a random array of manganese atoms on the surface, but rather consisted of an alternating "up and down" spatial arrangement of Mn atoms extending from the HOPG surface due to hydrogen bonding of the quinonoid complexes. We also showed that the topology of metal atoms on the surface could be controlled through the use of quinonoid metal complexes. A quinonoid rhodium complex showed catalytic activity in Suzuki-Miyaura type reaction. As a result of the excellent stability of the homogeneous catalyst $[(\text{quinone})Rh(COD)]^-$ in water, we also successfully demonstrated catalyst recycling in 1,2- and 1,4-addition reactions. The compound $[(\text{quinone})Ir(COD)]^-$ showed significantly poorer catalytic activity in 1,4-addition reactions. Following upon the excellent coordination ability of the quinonoid rhodium complexes to metal centers, we synthesized organometallic coordination polymer nanocatalysts and silica gel-supported quinonoid rhodium catalysts, the latter using a surface sol-gel technique. The resulting heterogeneous catalysts showed activity in the stereospecific polymerization of phenylacetylene.

1. Introduction

Hydroquinones (HQ) are well-known to undergo reversible proton-coupled electron transfer to afford semiquinones (SQ) and quinones (Q). The η^6-bonded manganese tricarbonyl complexes of hydroquinone, catechol, and resorcinol are thermally stable and can undergo reversible coupled proton and electron transfer with concomitant ring slippage: $\eta^6 \rightarrow \eta^5$ and $\eta^5 \rightarrow \eta^4$.[1−3] The process can be explained as simultaneous

Published on the Web 06/07/2013 www.pubs.acs.org/accounts
10.1021/ar300353n

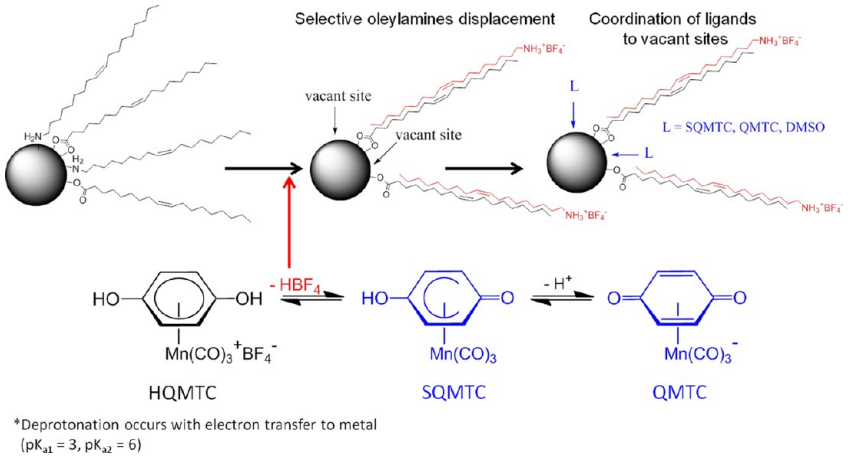

FIGURE 1. Surface modification of nanoparticles with [(η^6-hydroquinone)$Mn(CO)_3$][BF_4]. Reproduced with permission from ref 19. Copyright 2009 American Chemical Society.

deprotonation/oxidation of the quinonoid ring and reduction of the coordinated metal fragment. The electrophilic activation provided by the $Mn(CO)_3^+$ moiety results in [(η^6-hydroquinone)$Mn(CO)_3$]$^+$ (HQMTC) being quite acidic, showing lower pK_a (ca. 3) than that of free hydroquinone (pK_a ca. 10).[23,25] [(η^5-Semiquinone)$Mn(CO)_3$] complexes (SQMTC) form hydrogen-bonding-based supramolecules through self-assembly reactions.[3] Additionally, [(η^4-quinone)$Mn(CO)_3$]$^-$ complexes (QMTC) can form coordination polymers by binding metal ions through quinone oxygen atoms.[4−8]

Coordination polymers have been an active area of research for over 50 years. However, in recent years, the study of low-dimensional coordination polymers has been increasingly supplanted by the study of highly networked metal−organic frameworks (MOFs).[12−14] Prior to 2001,[4−8] all spacer/linker molecules used in the formation of reported coordination networks were simple organic molecules.[12−14] The essential improvement of metal−organometallic coordination networks[15−18] over simple coordination polymers or MOFs is associated with the presence of metals *both* in the backbone and on spacer ligands in the former. Herein we refer to doubly deprotonated η^4-quinone complexes as "organometalloligands"[5] because they not only coordinate to metal ions, acting as spacers/linkers, but are themselves π-bonded complexes with pendant metal centers.[4−11] A variety of coordination network structures has now been generated using organometalloligands.[4−8]

In this Account, we describe our recent progress in the applications of quinonoid metal complexes to coordination polymers,[23,33,37] surface chemistry,[19,27] and catalysts.[28,32,33,37,40,42] The aim of the Account is not only to demonstrate new applications of quinonoid metal complexes, but also to provide new insights into the formation of functional hybrid materials, the design of functionalized surfaces, and the use of quinonoid organic molecules in designing organometallic catalysts.

2. Manganese Quinonoid Complexes

2.1. Surface Modification of Fe_3O_4 with Manganese Quinonoid Complexes. Highly monodisperse magnetic NPs are commonly prepared via thermal decomposition of organometallic compounds in the presence of oleic acid and oleylamine, which serve as surfactants and permit good control of size, shape, composition, and internal structure. We have now demonstrated that magnetic NPs such as those of Fe_3O_4 and FePt, having oleylamine and oleic acid as surfactants on their surface,[20−22] can be surface-modified through the use of HQMTC. As a result, both bilayer formation and ligand exchange have been carried out simultaneously in a single pot, affording polar-surface magnetic NPs which are stable in polar solvents such as DMSO (Figure 1).[19]

This surface modification was achieved by agitation of a combined hexanes solution of the NPs and DMSO solution of HQMTC (Figure 2). Surface modification of the NPs caused their transfer from the hexanes to the DMSO layer. It is very likely that the protons from HQMTC play a role in this transfer. In fact, HQMTC equilibrates to SQMTC + HBF_4 in DMSO (Figure 1). To test the role of acid in this process,[19] nonprotic HQMTC analogue [(η^6-1,4-dimethoxybenzene)$Mn(CO)_3$][BF_4] was synthesized. Like the HQMTC, the dimethoxybenzene complex was soluble in DMSO; however, unlike HQMTC, it did not induce transfer of Fe_3O_4 NPs to the DMSO layer (Figure 2b).

HQMTC is readily deprotonated by the oleylamine to generate SQMTC. The surface sites generated by the

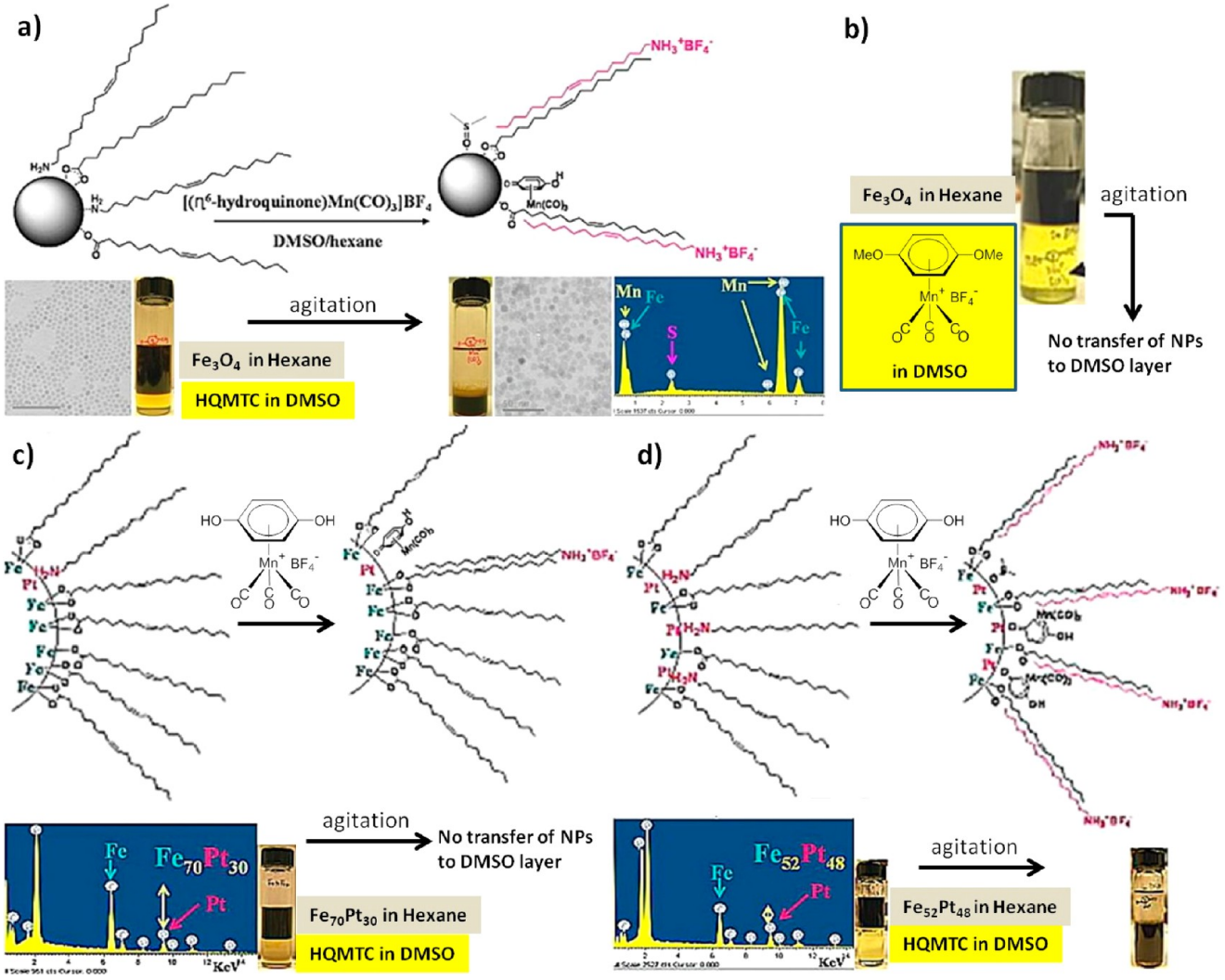

FIGURE 2. Proposed surface structure of NPs before and after surface modification: (a) Fe_3O_4 NP reaction with HQMTC, TEM image (scale bar: 100 nm (as-made Fe_3O_4 NPs, left) and 50 nm (surface modified Fe_3O_4 NPs, right)), and EDS spectrum of surface modified Fe_3O_4 NP; (b) Fe_3O_4 NP reaction with [(η^6-1,4-dimethoxybenzene)$Mn(CO)_3$][BF_4]; $Fe_{70}Pt_{30}$ (c) and $Fe_{52}Pt_{48}$ (d) reacted with HQMTC and EDS spectra of as-made NPs. Figure (a, c, d) adapted with permission from ref 19. Copyright 2009 American Chemical Society. Figure (b) reproduced from ref 23. Copyright 2009 John Wiley & Sons.

protonation of the oleylamine in this manner are then occupied by coordination of SQMTC and DMSO to the metal; peaks from Mn of SQMTC, Fe of Fe_3O_4 NP, and S of DMSO are apparent in the energy dispersive X-ray spectroscopy (EDS) spectrum (Figure 2a). The protonated oleylamine (oleylammonium tetrafluoroborate), participates in bilayer formation with alkyl chains of oleic acid molecules. The role of oleylamine in the surface modification of NPs, resulting in their solubility in polar solvents, was also confirmed for the surface modification of FePt NPs. It is known that oleic acid molecules are coordinated to Fe atoms at the surface of FePt NPs, while oleylamine molecules are coordinated to Pt atoms on the surface.[20,22] The Fe-rich $Fe_{70}Pt_{30}$ NPs have fewer Pt atoms at their surface in comparison with the generic $Fe_{52}Pt_{48}$ NPs, corresponding to greater relative Fe to Pt intensity in $Fe_{70}Pt_{30}$ compared to $Fe_{52}Pt_{48}$ by EDS. No transfer of $Fe_{70}Pt_{30}$ nanoparticles from the hexanes layer was observed (Figure 2c). From this result, it can be surmised that the amount of oleylamine coordinated to Pt atoms of the surface of FePt NPs is related to their solubility in DMSO after treatment with HQMTC. In contrast, treatment of $Fe_{52}Pt_{48}$ NPs with HQMTC enabled their partitioning from the hexanes to the DMSO layer (Figure 2d).

2.2. Incorporation of Fe_3O_4 Nanoparticles into Metal-Organometallic Coordination Polymers (3D). Extending this work, we have demonstrated that surface-modified Fe_3O_4 NPs can function as nuclei or templates for the generation of crystalline coordination polymers that contain Fe_3O_4 NPs (Figure 3).[23] The presence of Fe_3O_4 NPs offered the opportunity for facile separation of the hybrid material

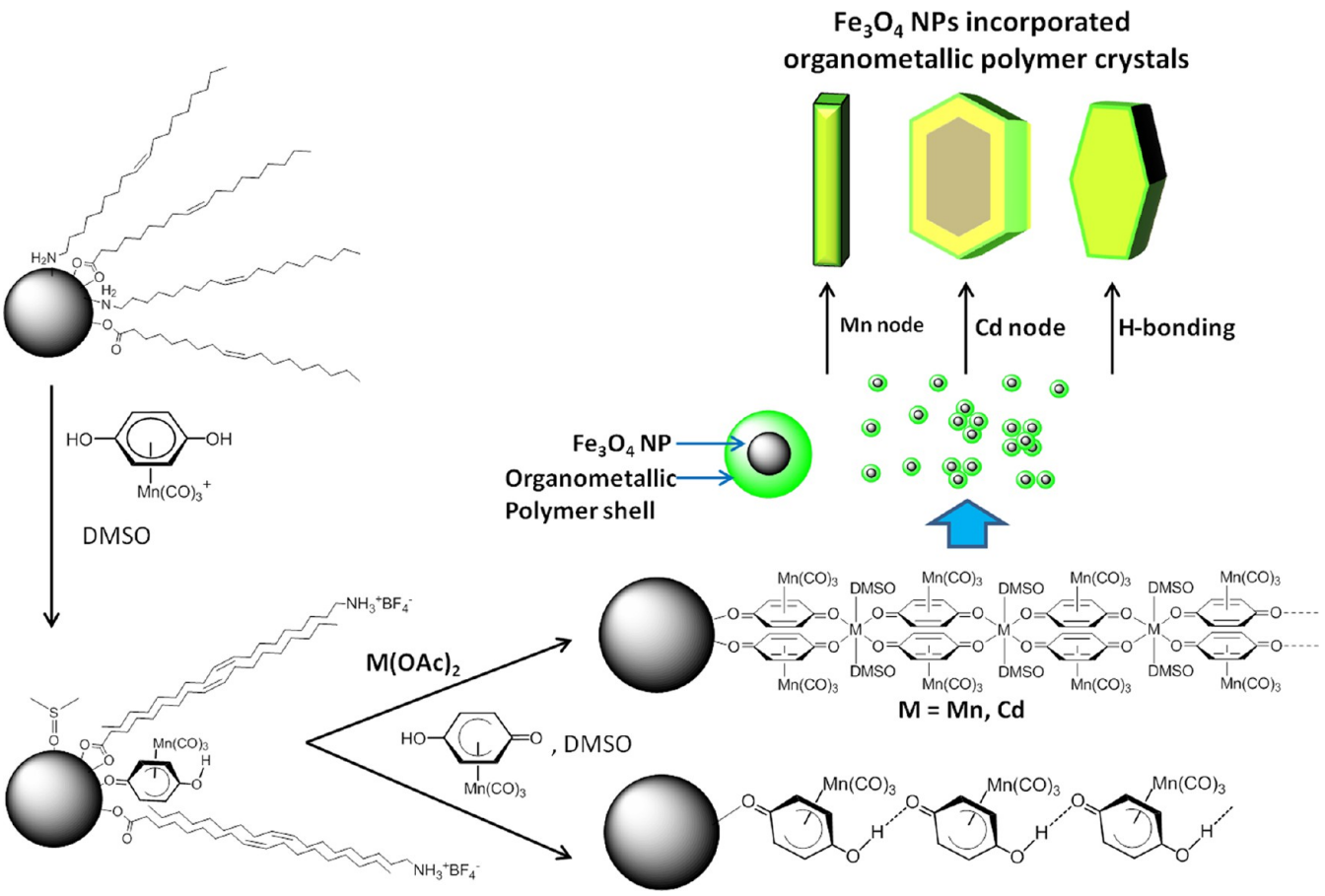

FIGURE 3. Surface modification of Fe_3O_4 NPs and formation of the metal-organometallic coordination polymers on the surface-modified NPs. Adapted with permission from refs 19 and 23. Copyright 2009 American Chemical Society and 2009 John Wiley & Sons.

via magnetic decantation. Therefore, we demonstrated that hybridized magnetic properties could be obtained by introducing paramagnetic metal nodes, such as Mn^{2+}, into coordination polymers (Figure 4f).[23]

Incorporation of Fe_3O_4 NPs into a polymer by a self-assembly process was accomplished by adding the surface-modified NPs to a solution of free SQMTC alone, or with $Mn(OAc)_2$ or $Cd(OAc)_2$, in DMSO. Crystals of both $[\{Mn(QMTC)_2(DMSO)_2\}_n]$-$Fe_3O_4$ NPs (Figure 4a–c) and $[(SQMTC)_n]$-Fe_3O_4 NPs (Figure 4d) were obtained.[23] The unique ability of the SQMTC molecules to bind to Fe on the NP surface through the C=O group and simultaneously present an OH group to form a hydrogen bond to excess SQMTC accounts for the resultant polymer formation. The Fe_3O_4 NP seen at the edge of the crystal has an organometallic shell consisting of $[\{Mn(QMTC)_2(DMSO)_2\}_n]$ (Figure 4c).

The magnetic properties of $[\{Mn(QMTC)_2(DMSO)_2\}_n]$-$Fe_3O_4$ NPs, $[(SQMTC)_n]$-Fe_3O_4 NPs, and $[\{Cd(QMTC)_2(DMSO)_2\}_n]$-$Fe_3O_4$ NPs were determined through the use of a vibrating sample magnetometer (VSM). SQMTC, QMTC, and Cd^{2+} are diamagnetic, while Mn^{2+} is paramagnetic and Fe_3O_4 NPs are superparamanetic. $[\{Mn(QMTC)_2(DMSO)_2\}_n]$-$Fe_3O_4$ NPs showed both paramagnetic and superparamagnetic behavior (Figure 4f). $[(SQMTC)_n]$-Fe_3O_4 NPs (Figure 4h) and $[\{Cd(QMTC)_2(DMSO)_2\}_n]$-$Fe_3O_4$ NPs (Figure 5d) showed superparamagnetic behavior. This incorporation of nanosized functional materials into coordination polymers could lead to the fabrication of complex multifunctional materials for drug-delivery, bioimaging, and so on, with applications in materials science and biotechnology.[15–18]

2.3. Patterned Monolayers of Functionalized Neutral and Charged Manganese Quinonoid Complexes on HOPG (2D). An advantageous property of quinonoid manganese complexes lies in their tunability. One aspect of this tunability is associated with the possibility of replacing one or more of the carbonyls with functionalized ligands. Alternatively, the arene itself can be functionalized. This twofold tunability allows the quinonoid manganese tricarbonyl system to be elaborated into a variety of modified forms. Thus, for example, although SQMTC itself has very limited solubility owing to intermolecular hydrogen bonding, it can be rendered highly soluble in organic solvents by

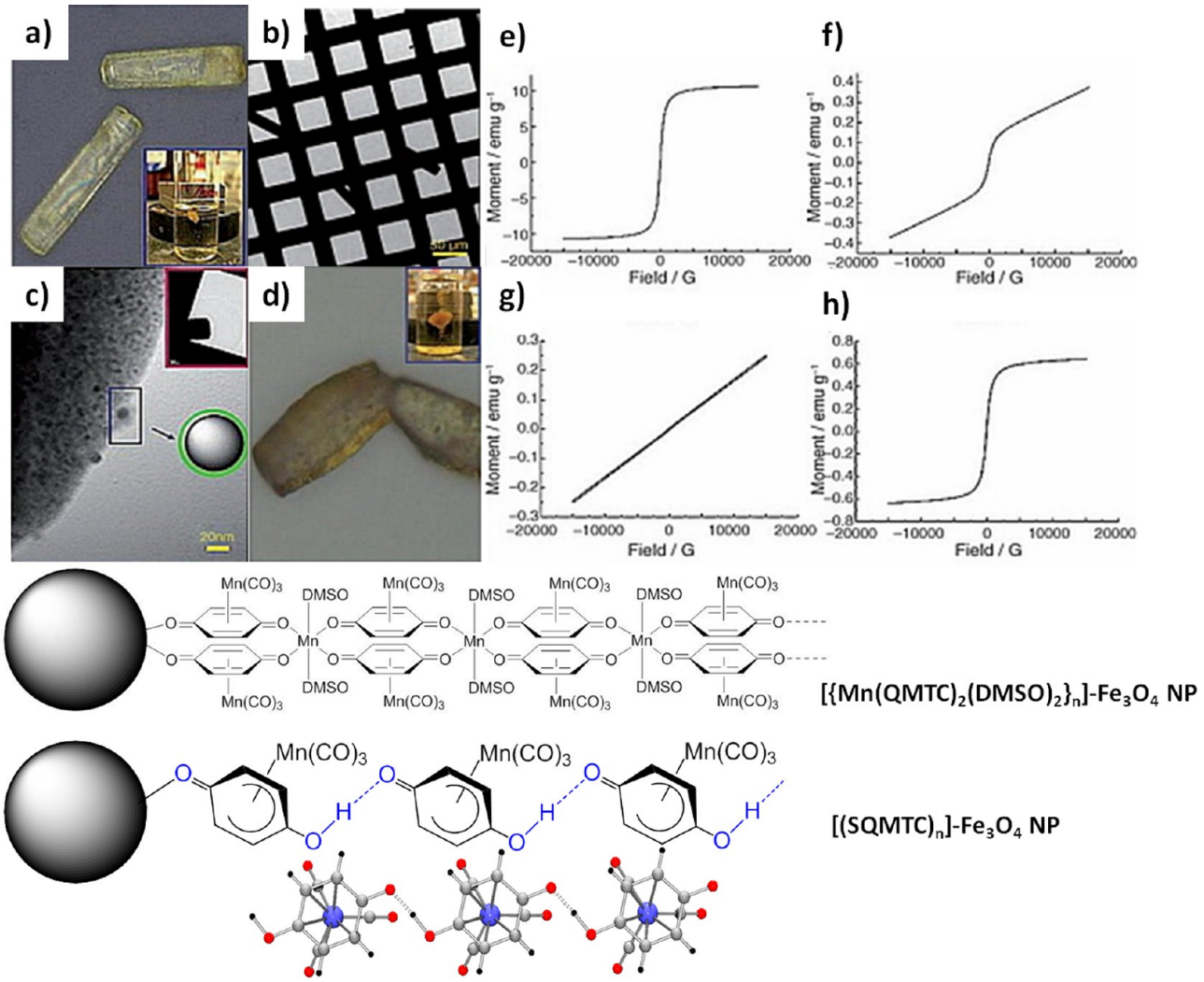

FIGURE 4. (a) Optical microscopy image of $[\{Mn(QMTC)_2(DMSO)_2\}_n]$-$Fe_3O_4$ NP crystals; (b) TEM image of $[\{Mn(QMTC)_2(DMSO)_2\}_n]$-$Fe_3O_4$ NP crystals on TEM grid; (c) TEM image (scale bar: 20 nm) of a Fe_3O_4 NP with a shell of $[\{Mn(QMTC)_2(DMSO)_2\}_n]$-$Fe_3O_4$ NP crystal; (d) optical microscope image of $[(SQMTC)_n]$-Fe_3O_4 NP crystal; magnetization curves of Fe_3O_4 NPs (e), $[\{Mn(QMTC)_2(DMSO)_2\}_n]$-$Fe_3O_4$ NP crystals (f), $[\{Mn(QMTC)_2(DMSO)_2\}_n]$ crystals (g), and $[(SQMTC)_n]$-Fe_3O_4 NP crystals (h). Reproduced from ref 23. Copyright 2009 John Wiley & Sons.

functionalization of the arene with long-chain alkyl substituents. Multifuctionality of the [(quinonoid)$Mn(CO)_3$] complexes, combined with other well-known interactions such as $\pi-\pi$ arene interaction with graphite, may be expected to enrich the practice of 2D surface nanostructure assembly.

Previous fabrications of metal−ligand complex nanostructures on surfaces have, to our knowledge, all involved complexes bearing carboxylates, amine or pyridine nitrogen, or oxygen from ethers and alcohols as the ligand donor atoms.[24−26] There have been no reports of 2D nanostructure fabrication involving organometallic arene-bonded complexes. Such systems are especially interesting because the arene ligands are predisposed to interact with certain kinds of surfaces. In the case of HOPG, the graphite surface is likely to bind the organometallic species through $\pi-\pi$ interaction. With this in mind, we prepared [(η^5-2,5-didodecoxy-1,4-semiquinone)$Mn(CO)_3$] on HOPG and studied the 2D structure of the product by scanning tunneling microscopy (STM).[27]

Figure 6d and e depicts representative STM images of [(η^5-2,5-didodecoxy-1,4-semiquinone)$Mn(CO)_3$] on HOPG adsorbed at the interface between HOPG and a solution of [(η^5-2,5-didodecoxy-1,4-semiquinone)$Mn(CO)_3$] in phenyloctane. The distance between the rows seen was found to be 25 ± 1 Å (Figure 6e), roughly matching the intermolecular distance between arene manganese carbonyl moieties observed in the *ac* plane of the X-ray crystal structure, 22.3 Å (the length of the *c* axis in the unit cell, Figure 6b). It is reasonable that the distance between the rows (bright) differ somewhat from the intermolecular distance noted between

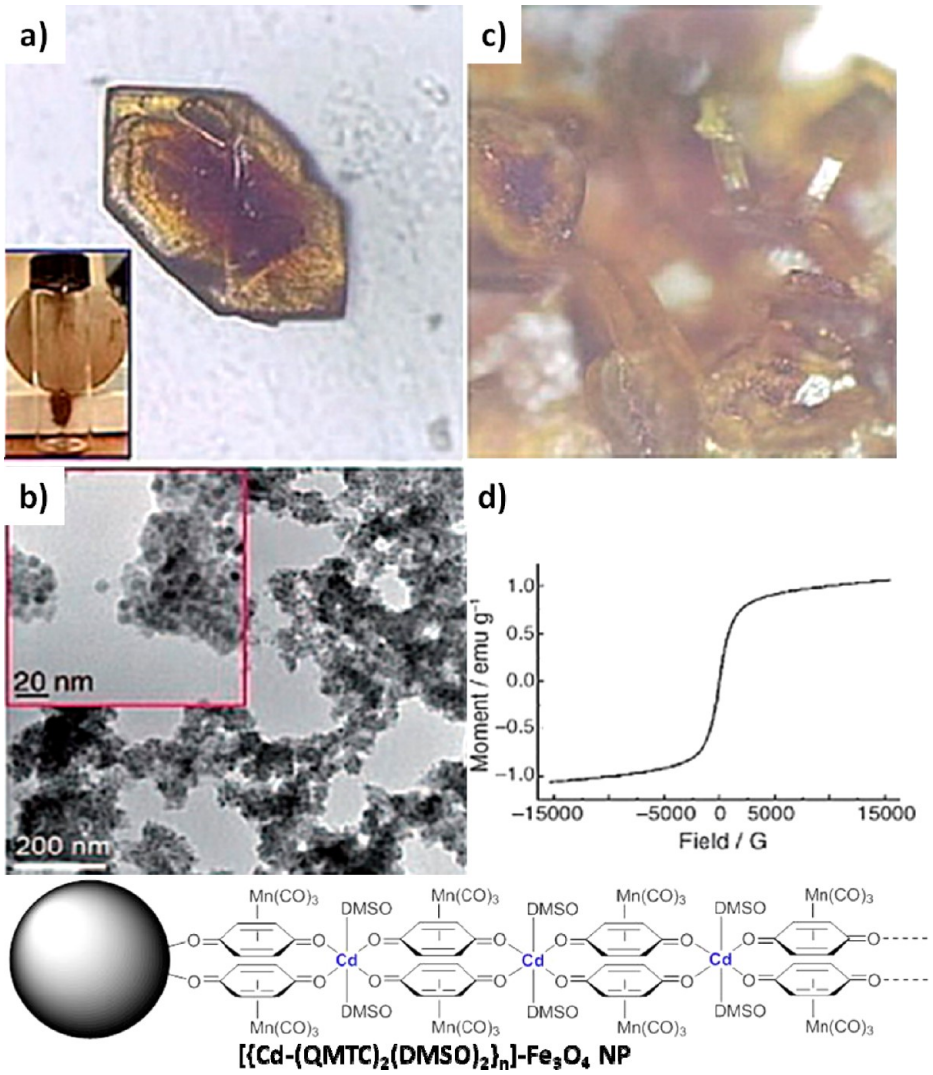

FIGURE 5. (a) Optical microscope image of a $[\{Cd(QMTC)_2(DMSO)_2\}_n]$-$Fe_3O_4$ NP crystal; (b) enlarged optical microscope image of $[\{Cd\text{-}(QMTC)_2(DMSO)_2\}_n]$-$Fe_3O_4$ NP crystals; (c) TEM image of the aggregated Fe_3O_4 NPs which have an organometallic coordination polymer shell formed during the crystallization process; (d) magnetization curve for $[\{Cd(QMTC)_2(DMSO)_2\}_n]$-$Fe_3O_4$ NP crystals. Reproduced from ref 23. Copyright 2009 John Wiley & Sons.

the SQMTC moieties along the *c* axis in the crystal. On the HOPG surface, an additional $\pi-\pi$ interaction is expected, which is not present in the crystalline state (3D structure).

The center-to-center distance between bright spots within the same row in the STM image is 11.3 ± 0.1 Å (Figure 6g). This distance is in good agreement with the value of 11.5 Å for the Mn···Mn distance between every other SQMTC moiety on the *a* axis of the crystal (Figure 6c). The reason why these distances are in agreement is probably associated with the difference in the height from the HOPG surface of the adjacent SQMTC moieties. In the crystal structure of [(η^5-2,5-didodecoxy-1,4-semiquinone)$Mn(CO)_3$] complex (Figure 6c), the Mn atoms in adjacent SQMTC groups are found to differ in elevation by roughly 2.4 Å, creating an alternating "up/down" sequence that repeats along the *a* axis (Figure 6c). It seems that the periodicity (11.3 ± 0.1 Å) in the STM image (Figure 6g) is related to visualization of the "higher" SQMTC moieties only.

[(η^6-1,4-Dioctyloxybenzene)$Mn(CO)_3$][BF_4] was synthesized for its inability to hydrogen-bond. In spite of its ionic charge and relatively short alkyl chains, [(η^6-1,4-dioctyloxybenzene)$Mn(CO)_3$][BF_4] was sufficiently soluble in phenyloctane to allow a monolayered 2D structure to form on HOPG (Figure 7a−c).[27] The center-to-center distance between adjacent arene manganese tricarbonyl moieties within rows is approximately 10 Å (Figure 7c). Because this 10 Å spacing is longer than normally expected for the distance between arenes, we focused on the location of

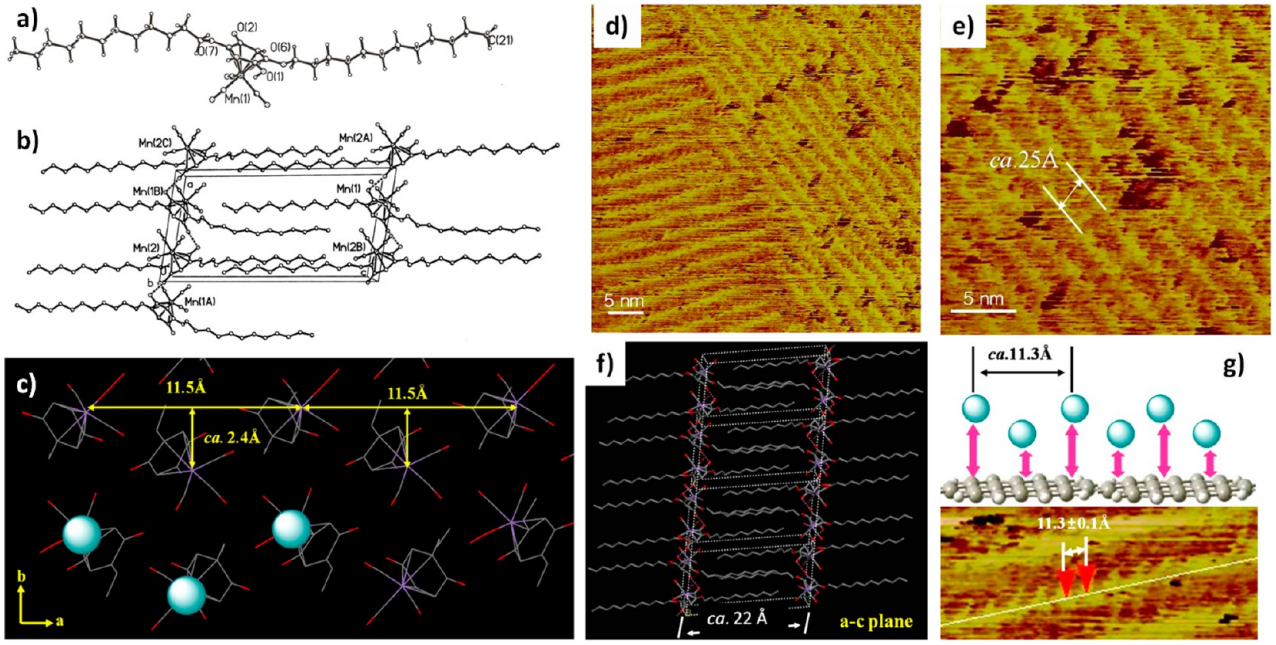

FIGURE 6. (a) Single-crystal X-ray structure of [Mn(η^5-2,5-didodecoxy-1,4-semiquinone)$(CO)_3$]; (b) spatial arrangement of the molecules in the *ac* plane in the crystal; (c) stacking of 2D layers along the *b* axis direction; (d) STM image of [(η^5-2,5-didodecoxy-1,4-semiquinone)Mn$(CO)_3$] on HOPG (25 °C, ambient pressure) at $I_{set} = 100$ pA and $V_{bias} = 1$ V. Large-scale STM image (50 × 50 nm^2); (e) enlarged STM image (25 × 25 nm^2); distance between the rows is ≈25 Å; (f) single-crystal X-ray structure of [(η^5-2,5-didodecoxy-1,4-semiquinone)Mn$(CO)_3$] viewed along the *a* and *c* axes (all hydrogen atoms omitted for clarity; C = gray, Mn = purple, O = red); (g) enlarged STM image (15 × 15 nm^2). Center-to-center distance between adjacent bright spots in a row = 11.3 ± 0.1 Å. Inset: schematic diagram of Mn atoms on the surface of HOPG. Reproduced from ref 27. Copyright 2009 John Wiley & Sons.

BF_4^- counterions in the 2D structure. Although the BF_4^- counterions could not be seen clearly in the STM image, it can be assumed that BF_4^- counterions play a role in connecting the positively charged complexes within rows by electrostatic interactions. The crystal structure of the [(η^6-1,4-dimethoxybenzene)Mn$(CO)_3$][BF_4] confirmed that the BF_4^- counterions are located between the cationic complexes and that the distance between Mn atoms along the *c* axis is 10.9 Å (Figure 7d). The Mn···Mn distance in the crystal is compatible with the center-to-center distance determined from the STM image.

3. Rhodium Quinonoid Complexes for Catalysis

3.1. Deprotonation of [(η^6-Hydroquinone)Rh(η^4-COD)][BF_4] Complexes. We have expanded the applications of π-bonded quinonoid manganese complexes by demonstrating behaviors such as metal-organometallic coordination network formation,[4−8] surface modification of NPs,[19] formation of coordination polymers on NPs,[23] and formation of 2D monolayered organometallic structures on HOPG.[27] However, the activity of quinonoid metal complexes as catalysts (inarguably one of the most significant applications of organometallic complexes) has not yet been studied. We reasoned that if organometalloligand complexes could be shown to function in catalysis, differences from, and perhaps advantages over, the use of simple organic ligands in organometallic complexes, metal−organic polymers, or MOFs might be uncovered. To explore the catalytic behavior of π-bonded quinonoid metal complexes, a hydroquinone complex of the catalytically active metal, Rh, was first considered. It was reasoned that the ability of a hydroquinone metal complex system to alter the charge on the metal by reversible deprotonation might provide a simple way to tune catalytic activity. The π-bonded hydroquinone rhodium complex was synthesized by the reaction of $[Rh(COD)Cl]_2$ with $AgBF_4$ and 1,4-hydroquinone (Figure 8).[28,31] The resulting [(η^6-hydroquinone)Rh(η^4-COD)][BF_4] underwent deprotonation to afford stable neutral [(η^5-semiquinone)Rh(η^4-COD)] and anionic [(η^4-quinone)Rh(η^4-COD)][M] (M = Li^+, K^+, Bu_4N^+) in organic solvents such as THF.[28,30] It was shown that the doubly deprotonated anionic η^4-quinone complex could function as organometalloligand either by bridging two discrete $\{Li_4O_4\}$ cubane units or by forming polymeric species by bridging $\{Li_2O_2\}$ units.[30] The key to the construction of the dimeric species, as well as the related polymeric

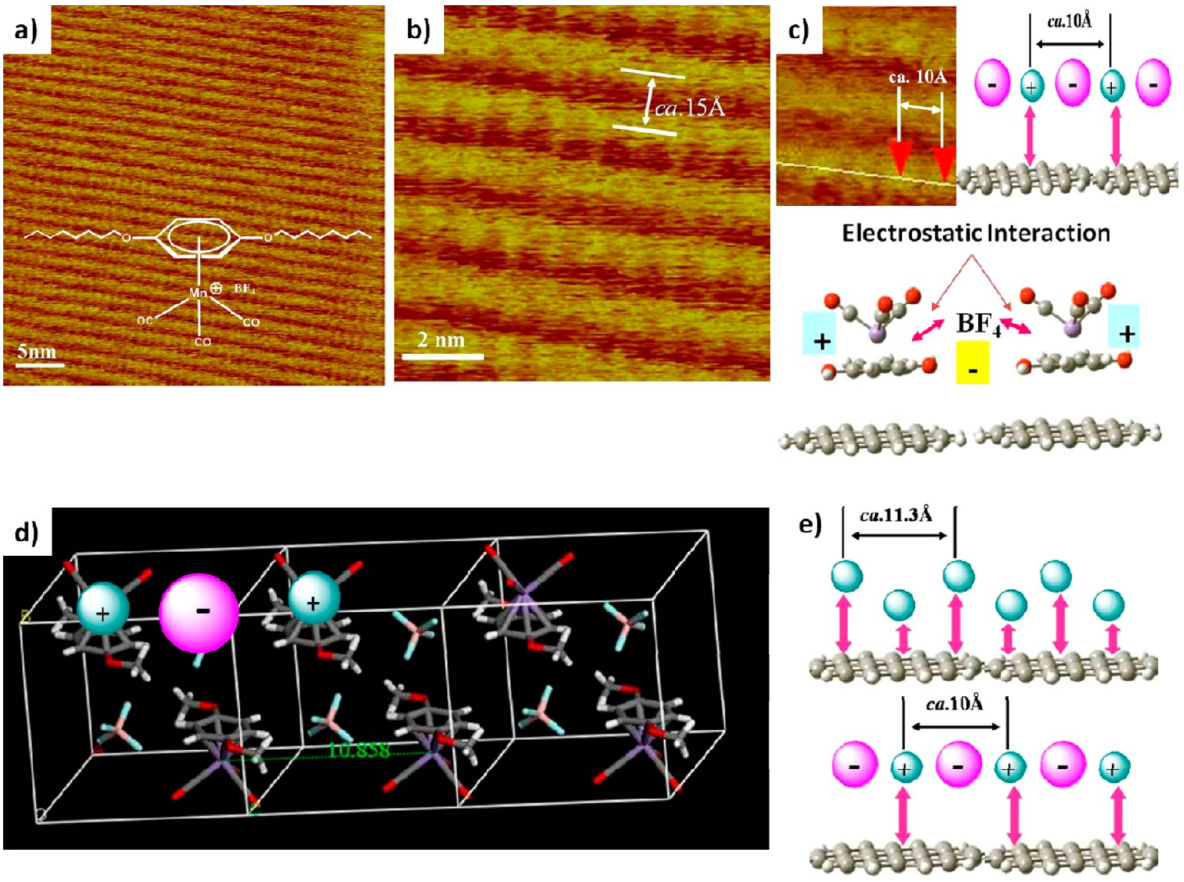

FIGURE 7. STM image of [(η^6-1,4-dioctyloxybenzene)Mn(CO)$_3$][BF$_4$] on HOPG (25 °C, ambient pressure) at I_{set} = 80 pA (constant current mode) and V_{bias} = 1 V: (a) large-scale image (41 × 41 nm^2), (b) enlarged image (10 × 10 nm^2), and (c) enlarged image (5 × 5 nm^2). The center-to-center distance between adjacent [Mn(η^6-1,4-dioctyloxybenzene)(CO)$_3$][BF$_4$] complexes is ≈10 Å. Inset: schematic diagram of Mn ions (small) and BF$_4^-$ counteranions (large) on the surface of HOPG. (d) Crystal structure of [(η^6-dimethoxybenzene)Mn(CO)$_3$][BF$_4$] (B = pink, C = gray, F = cyan, H = white, Mn = purple, O = red); (e) schematic diagram of Mn atoms of [(η^5-2,5-didodecoxy-1,4-semiquinone)Mn(CO)$_3$] complex (upper) vs Mn ions and BF$_4^-$ counterions of [(η^6-1,4-dioctyloxybenzene)Mn(CO)$_3$][BF$_4$] (bottom) on the surface of HOPG. Reproduced from ref 27. Copyright 2009 John Wiley & Sons.

species, is the ability of quinone oxygen atoms of [(η^4-quinone)Rh(η^4-COD)]$^-$ to function as ligands both within and external to the cubane aggregate itself.[30] As described below, the special character of [(η^4-quinone)Rh(η^4-COD)]$^-$ as an organometalloligand was readily applied to both coordination polymeric organometallic nanocatalysts[33,36,37] and silica gel-supported Rh catalysts.[38]

3.2. Rh Quinonoid Organometallic Nanospheres and Mn Quinonoid Core-Rh Quinonoid Organometallic Nanospheres and Their Catalytic Applications. Although the synthesis of nano- and microsized colloidal coordination networks[15−18] has been described, catalysis by organometallic-functionalized nanospheres[33,37] (formed by coordination polymerization of organometalloligands and metal) had yet to be demonstrated. We have now shown that nanosized metal−organometalloligand coordination polymers can be formed using [(η^4-quinone)Rh(η^4-COD)]$^-$ as an organometalloligand and that these materials are catalytically active. Treatment of [(η^6-hydroquinone)Rh(η^4-COD)][BF$_4$] with Al(O*i*-Pr)$_3$ in THF afforded an organometallic nanocatalyst (ON) material as an insoluble yellow solid,[33] along with 2-propanol (Figure 9a). This nanosized self-supported organometallic catalyst showed high catalytic activity (98% yield) in the stereoselective polymerization of phenylacetylene forming cis−transoidal polyphenylacetylene (cis-PPA).[34,35]

Because the active molecular catalytic sites of self-supported organometallic rhodium quinonoid nanospheres are present on the surface, the quinone rhodium species inside the sphere cannot participate in the catalysis. Therefore, in order to lessen the amount of expensive rhodium inside the nanosphere, organometallic core−shell nanospheres composed of cheaper Mn quinonoid cores and Rh quinonoid shells were prepared (Figure 9b).[37] The anionic QMTC was selected as the building block for use as the organometallic core in core−shell structured coordination polymer nanospheres consisting of Ti-QMTC core and

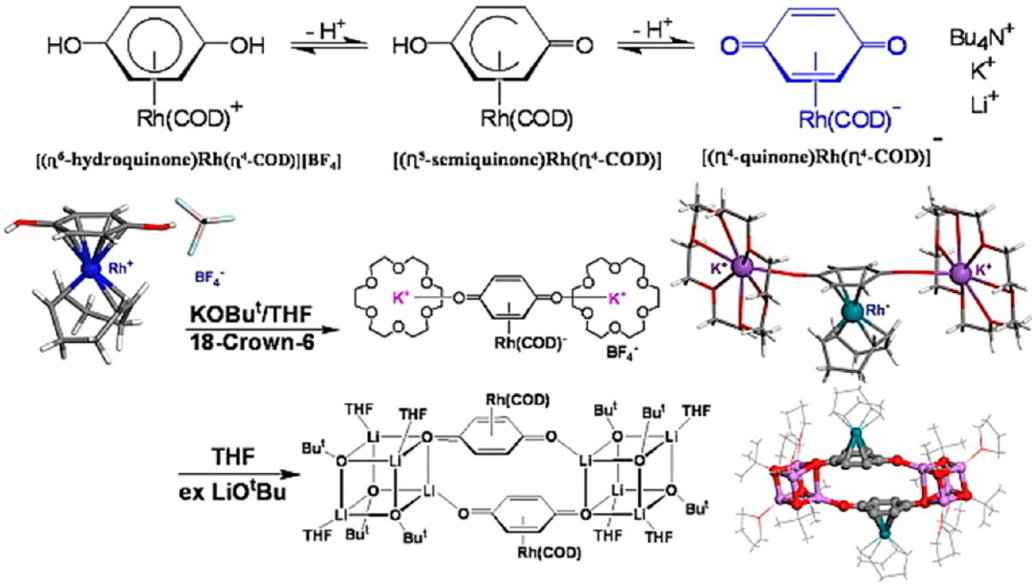

FIGURE 8. Deprotonation of [(η^6-hydroquinone)Rh(η^4-COD)][BF_4] in THF and crystal structures of its doubly deprotonated product, [(η^4-quinone)-Rh(η^4-COD)]$^-$ with [K(18-crown-6)]$^+$ and [Li_4(O^tBu)$_3$(THF)$_3$]$^+$. Middle figure adapted with permission from ref 28. Copyright 2005 American Chemical Society. Bottom figure reproduced from ref 30. Copyright 2005 John Wiley & Sons.

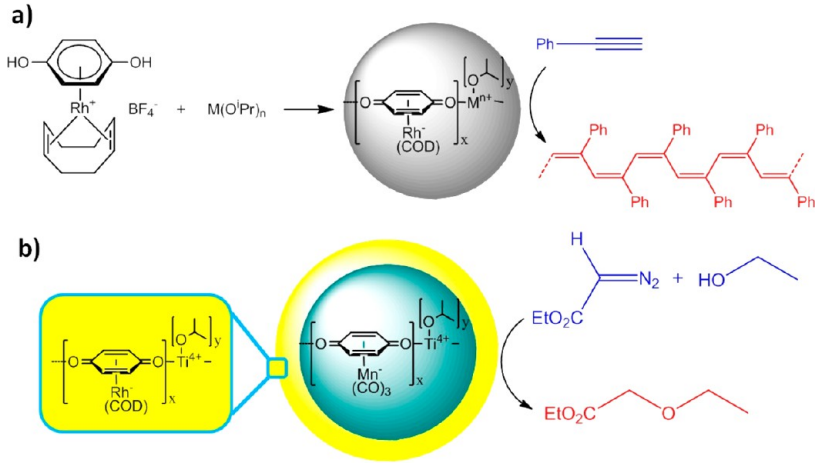

FIGURE 9. (a) Rhodium quinonoid organometallic nanosphere (M =Al, Ti). Adapted with permission from ref 33. Copyright 2006 American Chemical Society. (b) Mn quinonoid core-Rh quinonoid shell organometallic nanosphere. Adapted with permission from ref 37. Copyright 2007 Willey-VCH Verlag.

(Ti-[(η^4-quinone)Rh(η^4-COD)]$^-$ shell. The core–shell nanospheres showed excellent catalytic activity in the carbene transfer reaction of ethyl diazoacetate (EDA) to ethanol.

3.3. Silica-Supported Quinonoid Rhodium Catalysts. As described above, core–shell-type catalyst particles can be prepared having rhodium concentrated near the surface and cheaper quinonoid manganese tricarbonyl analogue in the interior. Nevertheless, even this type of core–shell type catalyst still contains a significant fraction of the rhodium located at sufficient depth (e.g., 15 nm in the 500 nm average size of core–shell nanosphere)[37] to preclude its participation in catalysis. To overcome this problem and maximize the catalytic activity per unit mass of rhodium, it would obviously be best to distribute the catalyst as a strict monolayer.[38] Recently, a surface sol–gel (SSG) methodology has been used for layer-by-layer functionalization of a silica surface via nonaqueous condensation of metal alkoxides with surface hydroxyl groups, followed by hydrolysis of the surface-bound metal alkoxides (Figure 10).[39] This methodology was adopted for the attachment of [(quinonoid)Rh(COD)] complexes to a silica-gel surface. This could be accomplished because the complexes experience the identical metal–organometalloligand coordination process at the surface of silica gel as occurs in the formation of

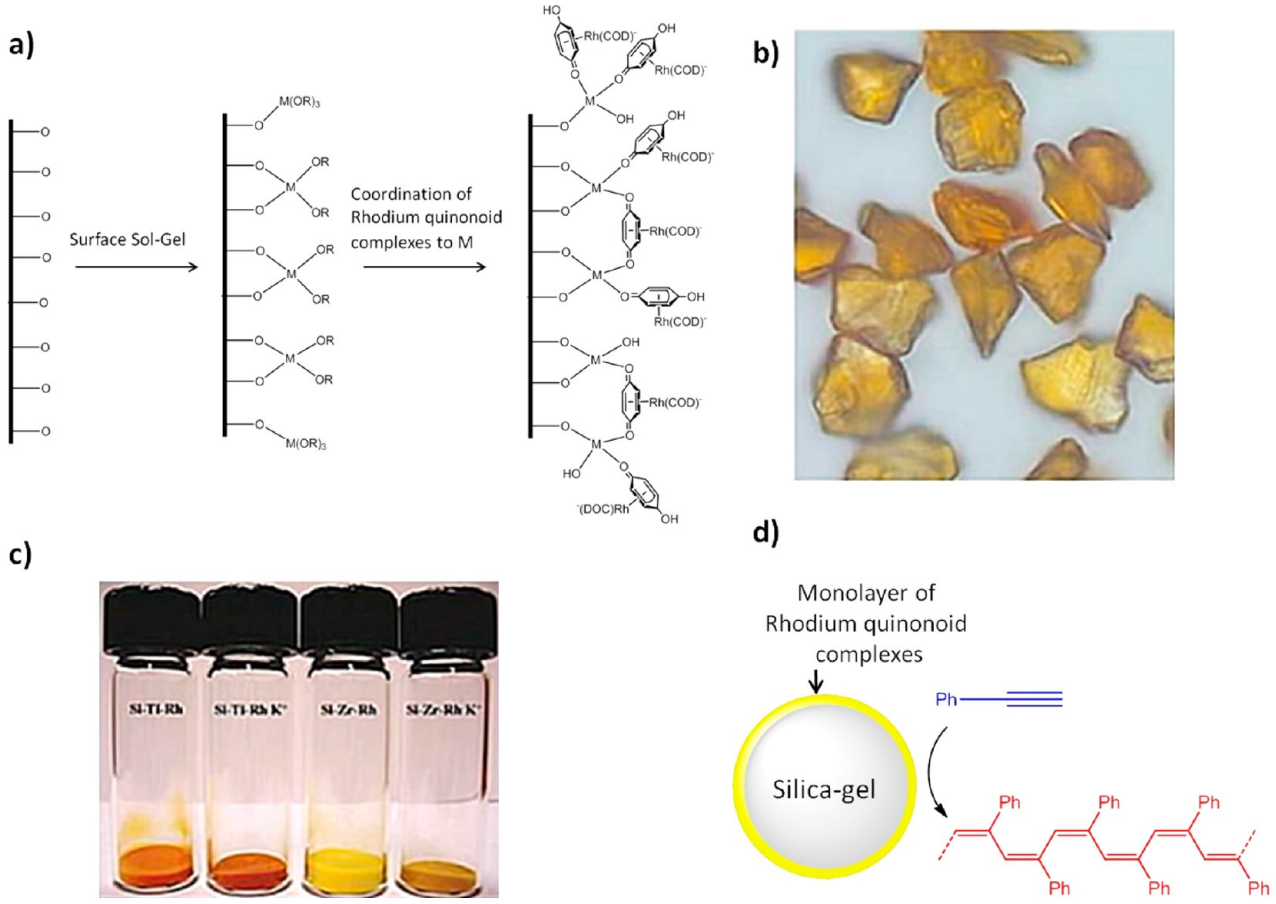

FIGURE 10. (a) Procedure for the fabrication of monolayered rhodium catalysts on a silica gel surface and plausible surface structure with Si−O-M(OR)$_3$ moieties (M = Ti, Zr; OR = OPr^i); (b) optical microscopy image of the Rh catalyst monolayered silica gel; (c) photograph of Si−Ti−Rh, Si−Ti−Rh$^-$K$^+$, Si−Zr−Rh, and Si−Zr−Rh$^-$K$^+$ catalysts (left to right); catalysts designated as Si−Ti−Rh−K$^+$ and Si−Ti−Rh−K$^+$ were formed on Si−Ti−Rh and Si−Zr−Rh by conversion of η^5 species on the surface to η^4 species by treatment with K$^+$^{t}BuO$^-$; (d) catalysis scheme for the polymerization of phenylacetylene. Figure (a,b,c) adapted with permission from ref 38. Copyright 2009 American Chemical Society.

coordination polymer nanospheres (whether organometallic nanocatalyst (ON) or core−shell nanosphere).

A variety of silica gel-supported Rh catalysts were prepared. All these catalysts produced higher yields and shorter *cis*-PPA chain lengths than did the free quinonoid Rh catalysts, which are heterogeneous in organic solvents. Both higher yield and shorter PPA chain length indicate that a larger number of Rh molecules is available for catalysis in the silica gel-supported systems than in the free quinonoid Rh catalysts.

3.4. Catalysis of 1,2- and 1,4-Addition Reactions. Based on the observation that anionic [(η^4-quinone)Rh(η^4-COD)][M] (M = Li$^+$, K$^+$, Bu$_4$N$^+$) is very soluble in water, its catalysis of the addition reaction of arylboronic acids to aldehydes in water was studied (Figure 11).[28,40] It was found that [(η^4-quinone)Rh(η^4-COD)][M] (M = Li$^+$, K$^+$) showed excellent catalytic activity, with alcohol product yields generally between 90% and 99%.

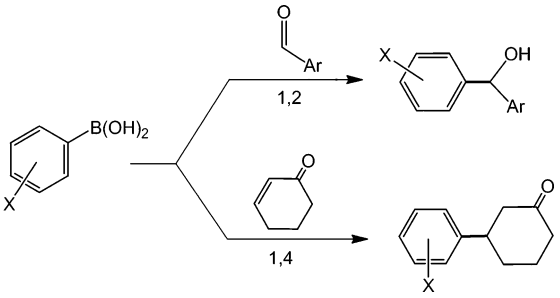

FIGURE 11. 1,2-Addition of arylboronic acid to aldehydes and 1,4-addition of arylboronic acid to activated olefinic acceptors.[28,32,40,42]

It is known that Suzuki-Miyaura type coupling reactions involving boronic acids are usually facilitated by the presence of stoichiometric external base. Recent theoretical studies suggest that the hard base OH$^-$ functions by binding to the electrophilic boron, and that this increases the rate of transmetalation.[29] In contrast, it is known that [(η^4-quinone)-Rh(η^4-COD)][M] (M = Li$^+$, K$^+$) are effective catalysts without

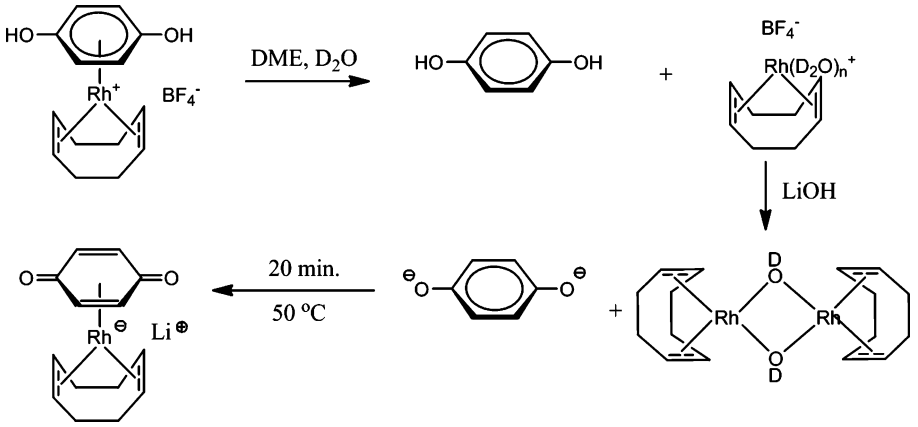

FIGURE 12. Formation of [(η^4-quinone)Rh(η^4-COD)][Li] in aqueous media. Reproduced with permission from ref 40. Copyright 2009 American Chemical Society.

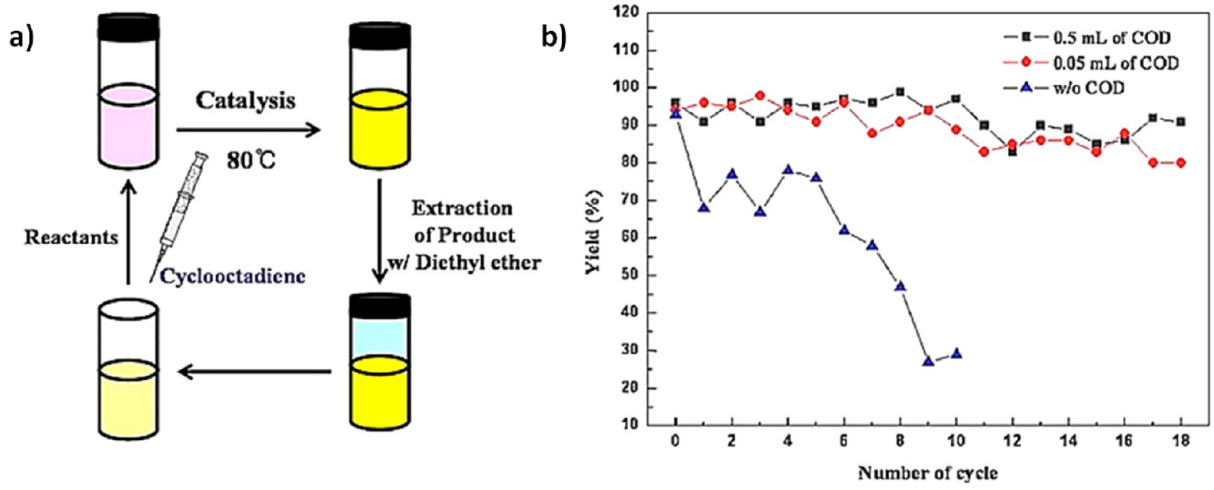

FIGURE 13. (a) Procedure for the recycle of [(η^4-quinone)Rh(η^4-COD)][Li] in 1,2- and 1,4-addition catalysis (solvent = water); (b) isolated yield of 1,4-addition catalysis upon repeat catalytic cycles. Figure (b) reprinted with permission from ref 40. Copyright 2009 American Chemical Society.

the need for external base.[28] Based on this information, it can reasonably be concluded that the [(η^4-quinone)Rh(η^4-COD)]$^-$ complex itself functions as the base, much like OH$^-$, by binding to the boron via quinonoid oxygens. Thus, multifunctionality is demonstrated for the organometalloligand [(η^4-quinone)Rh(η^4-COD)]$^-$ complex in the catalysis of 1,2-addition reactions. It not only facilitates the rate of transmetalation of arylboronic acids by binding of the quinonoid oxygen to the electrophilic boron, but also catalyzes the coupling reaction through the action of Rh, which is π-bonded to the quinonoid ligand.

In like fashion, [(η^4-quinone)Rh(η^4-COD)]$^-$ complexes were also applied to the catalysis of 1,4-addition reactions of arylboronic acids to the electron-deficient olefin, 2-cyclohexen-1-one.[32] In this case, the catalysis was performed in situ instead of using premade [(η^4-quinone)Rh(η^4-COD)][M] (M = Li$^+$, K$^+$). Thus, [(η^6-hydroquinone)Rh(η^4-COD)][BF$_4$], LiOH, and the mixed water and dimethoxyethane (DME) solvent were combined with the substrates, and the reaction mixture was heated at 50 °C. It was observed that catalysis of the 1,4-addition reaction of arylboronic acids with electron-deficient olefins, such as 2-cyclohexen-1-one, was highly efficient.

For comparison, [(η^6-hydroquinone)Ir(η^4-COD)][BF$_4$] was synthesized and its doubly deprotonated product, [(η^4-quinone)Ir(η^4-COD)]$^-$ complex, was applied to the catalysis of the 1,4-addition reaction of arylboronic acids to the several kinds of electron-deficient olefins.[42] However, the iridium complex failed to show as great catalytic activity as that of its rhodium counterpart.

In our original report of the catalysis of 1,2-addition reaction of arylboronic acids to aldehydes by quinone rhodium complexes,[28] the presumed mechanism was based on the assumption that [(η^4-quinone)Rh(η^4-COD)][M]

(M = Li^+, K^+) complexes would survive the reaction conditions (water, heating). What is more, in our report of 1,4-addition reaction catalysis of arylboronic acids with electron-deficient olefins,[32] it was assumed that [(η^6-hydroquinone)Rh(η^4-COD)][BF_4] was transformed to [(η^4-quinone)Rh(η^4-COD)][Li] in aqueous solvent, thus generating anionic Rh species that were thermally stable. However, at that time, we did not demonstrate which Rh species actually exist under the catalytic conditions used. Using ^{1}H NMR, we have since been able to ascertain the likely species present during the reaction.[40,41] It was observed that [(η^4-quinone)-Rh(η^4-COD)][M] (M = Li^+, K^+) complexes obtained via deprotonation in THF indeed remain stable in aqueous conditions either at room temperature or under heating, and also that aqueous [(η^6-hydroquinone)Rh(η^4-COD)][BF_4] can be converted to [(η^4-quinone)Rh(η^4-COD)][Li] by LiOH (Figure 12).[40]

3.5. Recycling of the Rhodium Quinone Complex in 1,2- and 1,4-Addition Catalysis. We showed that [(η^4-quinone)-Rh(η^4-COD)][M] (M = Li^+, K^+) is stable under catalytic conditions (heat, aqueous solvent). Based on this remarkable stability, Rh catalyst recycling experiments were performed. Water was chosen for the reaction because it is a convenient and environmentally benign solvent that allows for ready product extraction into diethyl ether. Significantly, it was shown that the aqueous solution of [(η^4-quinone)Rh(η^4-COD)][Li] could be effectively recycled.[40] It was observed that the catalysis yield remained over 90% at seventh recycle in the 1,2-addition reaction. The isolated yields for the 1,4-addition of *p*-tolylboronic acid to 2-cyclohexen-1-one are given in Figure 13b. As in the case of recycling experiment of the 1,2-addition reaction, it was observed that addition of COD and LiOH after each run prevented a substantial drop-off in yield. Without additional COD, the yield of product was observed to be 68% for the first recycle and only 29% for the 10th recycle. Thus, it appears that the COD ligand is labile during the catalysis reaction, and its replenishment is important.

4. Summary

This Account has examined the properties and uses of quinonoid metal complexes. Deprotonation of OH in HQMTC due to electron withdrawal by $Mn(CO)_3$ enabled surface modification of NPs. The resulting NPs were used as nuclei for encapsulation in coordination polymer shells. The hydrogen bond angle in SQMTC produced a unique "up and down" self-assembled topology of Mn atoms on the HOPG surface. Deprotonation of quinonoid rhodium or iridium complexes produced heterogeneous and homogeneous catalysts for organic reactions. Thus, the versatile quinonoid metal system reviewed in this Account offers useful options and mechanistic insight in the design of functional organometallic molecules.

We are grateful to the donors of the Petroleum Research Fund, to the National Science Foundation (CHE-0308640), and to Brown University (Vincent-Wernig Fellowship, Corinna Borden Keen Research Fellowship, and Dean Peder Estrup Graduate Student Research Fellowship) for support of this research. We thank Prof. Shouheng Sun (nanochemistry), Prof. Matthew B. Zimmt (STM), and Prof. Gene B. Carpenter (X-ray Crystallography) in the Chemistry Department, Brown University for their support. We also extend our appreciation to Johnson-Matthey for the loan of $RhCl_3$ through the Johnson-Matthey Precious Metals Loan Program.

Note Added after ASAP Publication. This paper was published on the Web on June 7, 2013. Figure 4 was corrected and the revised version was reposted on June 12, 2013.

BIOGRAPHICAL INFORMATION

Sang Bok Kim received his B.S. from Dankook University in 1997, M.S. from Seoul National University in 2000, and after working at Korea Institute of Science and Technology, enrolled at Brown University in 2003, receiving his Ph.D. under Prof. Dwight Sweigart in 2009. He carried out postdoctoral fellow work at Georgia Institute of Technology and has been a postdoctoral fellow under Prof. Roy Gordon at Harvard University since 2010.

Robert D. Pike is the Floyd Dewey Gottwald Sr. Professor of Chemistry at the College of William & Mary. Prof. Pike received his B.S. from The George Washington University in 1982, and after working at Monsanto Co. for 3 years, enrolled at Brown University, receiving his Ph.D. under Prof. Dwight Sweigart in 1991. In his 20 years at William & Mary, Prof. Pike has worked with nearly 100 undergraduate research students and published nearly 100 papers. His research is in the areas of metal−organic networks, organometallics, coordination chemistry, and X-ray crystallography.

Dwight A. Sweigart received his B.A. from Franklin and Marshall College in 1967 and his Ph.D. in chemistry from Northwestern University in 1971 under Prof. R. G. Pearson. He carried out postdoctoral work under NATO fellowships at Oxford University and the University of Wales (Cardiff). He was appointed assistant, and then associate, professor of chemistry at Swarthmore College, and in 1980 moved to Brown University, attaining the rank of full professor of chemistry in 1987. He is the author of over 180 scientific papers and mentored 30 doctoral students. He was the recipient of numerous awards and served as associate editor of *Organometallics* 1997−2010. He passed away in October 2012.

FOOTNOTES

*To whom correspondence should be addressed. E-mail: skim01@fas.harvard.edu.
The authors declare no competing financial interest.
‖Dedicated to the memory of Prof. Dwight A. Sweigart, dedicated chemist, educator, mentor, and friend.

REFERENCES

1 Kim, S. B.; Lotz, S.; Sweigart, D. A. Supramolecular Materials: Metal-Quinonoid Complexes in Nanomaterials. *Inorganic and Bioinorganic Perspectives*; Lukehart, C. M., Scott, R. A., Eds.; John Wiley& Sons Ltd: Chichester, UK, 2008; pp 775−788.

2 Sun, S.; Carpenter, G. B.; Sweigart, D. A. η^6-Hydroquinone and Catechol Complexes of Manganese Tricarbonyl. Molecular Structure of $[(\eta^6\text{-hydroquinone})Mn(CO)_3]_2SiF_6$. *J. Organomet. Chem.* **1996**, *512*, 257–259.

3 Oh, M.; Carpenter, G. B.; Sweigart, D. A η^5-Semiquinone and η^4-Quinone Complexes of Manganese Tricarbonyl. Intermolecular Hydrogen Bonding in the Solid State and in Solution. *Organometallics* **2002**, *21*, 1290–1295.

4 Oh, M.; Carpenter, G. B.; Sweigart, D. A. Metal-Mediated Self-Assembly of π-Bonded Benzoquinone Complexes into Polymers with Tunable Geometries. *Angew. Chem., Int. Ed.* **2001**, *40*, 3191–3194.

5 Oh, M.; Carpenter, G. B.; Sweigart, D. A. Self-Assembly Using Organometalloligands as Spacers in the Controlled Formation of Isomeric 1D and 2D Supramolecular Quinonoid. Networks. *Angew. Chem., Int. Ed.* **2002**, *41*, 3650–3653.

6 Oh, M.; Carpenter, G. B.; Sweigart, D. A. Supramolecular Metal-Organometallic Coordination Networks Based on Quinonoid π-Complexes. *Acc. Chem. Res.* **2004**, *37*, 1–11.

7 Oh, M.; Reingold, J. A.; Carpenter, G. B.; Sweigart, D. A. Manganese Tricarbonyl Transfer (MTT) Reagents in the Construction of Novel Organometallic Systems. *Coord. Chem. Rev.* **2004**, *248*, 561–569.

8 Reingold, J. A.; Son, S. U.; Kim, S. B.; Dullaghan, C. A.; Oh, M.; Frake, P. C.; Carpenter, G. B.; Sweigart, D. A. Pi-Bonded Quinonoid Transition-Metal Complexes. *Dalton Trans.* **2006**, 2385–2398.

9 Moussa, J.; Amouri, H. Supramolecular Assemblies Based on Organometallic Quinonoid Linkers: A New Class of Coordination Networks. *Angew. Chem., Int. Ed.* **2008**, *47*, 1372–1380.

10 Amouri, H.; Moussa, J.; Renfrew, A. K.; Dyson, P. J.; Rager, M. N.; Chamoreau, L.-M. Discovery, Structure, and Anticancer Activity of an Iridium Complex of Diselenobenzoquinone. *Angew. Chem., Int. Ed.* **2010**, *49*, 7530–7533.

11 Damas, A.; Ventura, B.; Moussa, J.; Esposti, A. D.; Chamoreau, L.-M.; Barbieri, A.; Amouri, H. Turning on Red and Near-Infrared Phosphorescence in Octahedral Complexes with Metalated Quinones. *Inorg. Chem.* **2012**, *51*, 1739–1750.

12 Eddaoudi, M.; Molder, D. B.; Li, H.; Chen, B.; Reineke, T. M.; O'Keeffe, M.; Yaghi, O. M. Modular Chemistry: Secondary Building Unit as a Basis for the Design of Highly Porous and Robust Metal-Organic Carboxylate Frameworks. *Acc. Chem. Res.* **2001**, *34*, 319–330.

13 Desiraju, G. R. Chemistry Beyond the Molecule. *Nature* **2001**, *412*, 397–400.

14 Moulton, B.; Zaworotko, M. J. From Molecules to Crystal Engineering: Supramolecular Isomerism and Polymorphism in Network Solids. *Chem. Rev.* **2001**, *101*, 1629–1658.

15 Oh, M.; Mirkin, C. A. Chemically Tailorable Colloidal Particles from Infinite Coordination Polymers. *Nature* **2005**, *438*, 651–654.

16 Imaz, I.; Hernando, J.; Ruiz-Molina, D.; Maspoch, D. Metal-Organic Spheres as Functional System for Guest Encapsulation. *Angew. Chem., Int. Ed.* **2009**, *48*, 2325–2329.

17 Champness, N. R. Coordination Polymers: From Metal- Organic Frameworks to Spheres. *Angew. Chem., Int. Ed.* **2009**, *48*, 2274–2275.

18 Lin, W.; Rieter, W. J.; Taylor, K. M. L. Modular Synthesis of Functional Nanoscale Coordination Polymers. *Angew. Chem., Int. Ed.* **2009**, *48*, 650–658.

19 Kim, S. B.; Cai, C.; Kim, J.; Sun, S.; Sweigart, D. A. Surface Modification of Fe_3O_4 and FePt Magnetic Nanoparticles with Organometallic Complexes. *Organometallics* **2009**, *28*, 5341–5348.

20 Sun, S. Recent Advances in Chemical Synthesis, Self-Aseembly, and Applications of FePt Nanoparticles. *Adv. Mater.* **2006**, *18*, 393–403.

21 Sun, S.; Zeng, H.; Robinson, D. B.; Raoux, S.; Rice, P. M.; Wang, S. X.; Li, G. Monodisperse MF_2O_4 (M = Fe, Co, Mn) Nanoparticles. *J. Am. Chem. Soc.* **2004**, *216*, 273–279.

22 Kim, J.; Rong, C.; Lee, Y.; Liu, J. P.; Sun, S. From Core/Shell Structured FePt/Fe_3O_4/MgO to Ferromagnetic FePt Nanoparticles. *Chem. Mater.* **2008**, *20*, 7242–7245.

23 Kim, S. B.; Cai, C.; Sun, S.; Sweigart, D. A. Incorporation of Fe_3O_4 NPs into Organometallic Coordination Polymer via NP Surface Modification. *Angew. Chem., Int. Ed.* **2009**, *48*, 2907–2910.

24 Barth, J. V.; Constantini, G.; Kern, K. Engineering Atomic and Molecular Nanostructure at Surfaces. *Nature* **2005**, *437*, 671–679.

25 Dmitriev, A.; Spillman, H.; Lin, N.; Berth, J. V.; Kern, K. Modular Assembly of Two-Dimensional Metal-Organic Networks at a Metal Surface. *Angew. Chem., Int. Ed.* **2003**, *42*, 2670–2673.

26 Langner, A.; Tait, S. L.; Lin, N.; Chandrasekar, R.; Ruben, M.; Kern, K. Ordering and Stabilization of Metal-Organic Coordination Chains by Hierarchical Assembly through Hydrogen Bonding at a Surface. *Angew. Chem., Int. Ed.* **2008**, *47*, 8835–8838.

27 Kim, S. B.; Pike, R. D.; D'Acchioli, J.; Walder, B. J.; Carpenter, G. B.; Sweigart, D. A. Patterned Monolayers of Neutral and Charged Functionalized Manganese Arene Complexes on an HOPG Surface. *Angew. Chem., Int. Ed.* **2009**, *48*, 1762–1765.

28 Son, S. U.; Kim, S. B.; Reingold, J. A.; Carpenter, G. B.; Sweigart, D. A. An Anionic Rhodium η^4-Quinoid Complex as a Multifunctional Catalyst for the Arylation of Aldehydes with Arylboronic Acid. *J. Am. Chem. Soc.* **2005**, *127*, 12238–12239.

29 Braga, A. A. C.; Morgon, N. H.; Ujaque, G.; Maseras, F. Computational Characterization of the Role of the Base in the Suzuki-Miyaura Cross-Coupling Reaction. *J. Am. Chem. Soc.* **2005**, *127*, 9298–9307.

30 Son, S. U.; Reingold, J. A.; Kim, S. B.; Carpenter, G. B.; Sweigart, D. A. Lithium Alkoxide $\{Li_4O_4\}$ Cubanes Bridged by Rhodium-Quinonoid Organometalloligands. *Angew. Chem., Int. Ed.* **2005**, *44*, 7710–7715.

31 Son, S. U.; Reingold, J. A.; Sweigart, D. A. Organometallic Crystal Engineering of [1,4- and 1,3-(hydroquinone)$Rh(P(OPh)_3)_2]BF_4$ by Charge Assisted Hydrogen Bonding. *Chem. Commun.* **2006**, 708–710.

32 Trenkle, W. C.; Barkin, J. L.; Son, S. U.; Sweigart, D. A. Highly Efficient 1,4-Additions of Electron-Deficient Aryl Boronic Acids with a Novel Rhodium(I) Quinonoid Catalyst. *Organometallics* **2006**, *25*, 3548–3551.

33 Park, K. H.; Jang, K.; Son, S. U.; Sweigart, D. A. Self-Supported Organometallic Rhodium Quinonoid Nanocatalysts for Stereoselective Polymerization of Phenylacetylene. *J. Am. Chem. Soc.* **2006**, *128*, 8740–8741.

34 Kishmoto, Y.; Eckerle, P.; Miyatake, T.; Noyori, R. Living Polymerization of Phenylacetylenes Initiated by $Rh(CCC_6H_5)$(2,5-norbornadiene)$[P(C_6H_5)_3]$. *J. Am. Chem. Soc.* **1994**, *116*, 1231–1232.

35 Falcon, M.; Farnetti, E.; Marsich, N. Stereoselective Living Polymerization of Phenylacetylene Promoted by Rhodium Catalysts with Bidentate Phosphines. *J. Organomet. Chem.* **2001**, *629*, 187–193.

36 Choi, J.; Yang, H. Y.; Kim, H. J.; Son, S. U. Organometallic Hollow Spheres Bearing Bis(N-Heterocyclic Carbene)-Palladium Species: Catalytic Application in Three Component Strecker Reactions. *Angew. Chem., Int. Ed.* **2010**, *49*, 7718–7722.

37 Park, K. H.; Jang, K.; Cho, Y.; Chun, J.; Kim, H. J.; Sweigart, D. A.; Son, S. U. Mn Quinonoid Core-Rh Quinonoid Shell Organometallic Nanosphere as Atom Economical Semiheterogeneous Catalysts in Carbene Transfer Reaction. *Adv. Mater.* **2007**, *19*, 2547–2551.

38 Kim, S. B.; Cai, C.; Trenkle, W. C.; Sweigart, D. A. Immobilization of Quinonoid Rhodium Catalyst on Silica-Gel Support by Surface Sol-Gel Process and its Catalytic Activity for Phenylacetylene Polymerization. *Organometallics* **2009**, *28*, 3000–3003.

39 Yan, W.; Mahurin, S. M.; Overbury, S. H.; Dai, S. Nanoengineering Catalyst Supports via Layer-by-Layer Surface Functionalization. *Top. Catal.* **2006**, *39*, 199–212.

40 Kim, S. B.; Cai, C.; Faust, M. D.; Trenkle, W. C.; Sweigart, D. A. Water Stable Organometallic Rhodium Quinone Catalyst and its Recyclability. *Organometallics* **2009**, *28*, 2625–2628.

41 Uson, R.; Oro, L. A.; Cabeza, J. A. Dinuclear Methoxy, Cyclooctadiene, and Barrelene Complexes of Rhodium (I) and Iridium (I). *Inorg. Synth.* **1985**, *23*, 126–130.

42 Kim, S. B.; Cai, C.; Faust, M. D.; Trenkle, W. C.; Sweigart, D. A. Synthesis and Catalytic Activity of Iridium Quinonoid Complexes. *J. Organomet. Chem.* **2009**, *694*, 52–56.